Int. J. Solids Structures Vol. 24, No. 11, pp. 1159–1173, 1988
Printed in Great Britain.

0020–7683/88 $3.00+ .00

STRAIN-CONTROLLED CREEP RUPTURE ANALYSIS OF A BEAM ON WINKLER FOUNDATION

RANDY J. GU
Department of Mechanical Engineering, Oakland University,
Rochester, MI 48309-4401, U.S.A

and

FRANCIS A. COZZARELLI
Department of Mechanical and Aerospace Engineering, State University of New York
at Buffalo, Buffalo, NY 14260, U.S.A.

(*Received* 2 *February* 1988; *in revised form* 5 *May* 1988)

Abstract—Based on the previously proposed uniaxial strain-controlled creep damage law, a continuum mechanical creep rupture analysis is carried out for a beam resting on a high temperature elastic Winkler foundation. The analysis includes the determination of the non-dimensional time for initial rupture, the propagation of the rupture front with the associated thinning of the beam, and the influence of creep damage on the deflection of the beam.

1. INTRODUCTION AND PROBLEM STATEMENT

Recently, scientists have observed a close relation between density change and the nucleation and growth of voids and microcracks associated with creep damage in polycrystalline materials. Extensive efforts have thus been made to identify and quantify creep damage in terms of the density variation which is attributed to cavitation in a creeping material. Following this concept, Piatti *et al.* (1977) developed a refined experimental technique to measure the density variation for use as a definition of creep damage. Using data obtained in this manner for steel, Belloni *et al.* (1977, 1980) proposed a statistically-based damage law at constant stress σ_0 and at time t in the power form for the uniaxial tension test

$$D = C\varepsilon_c^{\alpha}\sigma_0^{\gamma}t^{\delta} \tag{1}$$

where $D = -\Delta\rho/\rho_0$, ρ_0 is the density of the material in the virgin state, and $\Delta\rho$ the change in density due to the volume dilation of the material. In eqn (1) ε_c denotes the creep strain, and the material constants, α, γ, δ appear to be relatively insensitive to temperature, but C is highly sensitive to temperature T. The above damage law is analogous to the one presented in Woodford's parametric study of creep damage (Woodford, 1969). Because of its inherent mathematical complexity, the creep damage law proposed in Belloni *et al.* (1977, 1980) is somewhat inconvenient for analytical treatment within the framework of continuum creep damage mechanics. By introducing some assumptions based on experimental observation, a simplified uniaxial strain-controlled damage law is proposed (Gu and Cozzarelli, 1988)

$$D = C_0\varepsilon_s^{\alpha+\delta} \tag{2}$$

in which C_0 is a temperature independent material constant, and ε_s the steady-state creep strain. Here, the material is assumed to be fully dominated by Norton's steady creep law under constant uniaxial tensile stress σ_0

$$\dot{\varepsilon}_s = A(T)\sigma_0^n \tag{3}$$

in which n is the constant stress power, and $A(T)$ the temperature sensitive reciprocal viscosity coefficient. In analogy with Kachanov's damage variable ω (Kachanov, 1961), the

damage D has a value equal to zero in the virgin state and is equal to a critical value at rupture D_r, which is a material constant. Note that, although damage is an explicit function of strain alone, it is an implicit function of temperature and stress via creep constitutive law (3). In accordance with eqn (2), a material exposed to stress experiences damage directly related to the creep strain, and rupture occurs as the available creep ductility is exhausted.

The extension of the original creep damage law, eqn (1), to the case of time-dependent uniaxial stress has been presented in Cozzarelli and Bernasconi (1981). In the case of simplified eqn (2) it suffices to employ the integral form of creep strain for variable stress, and thus integrating $\dot{\varepsilon}_s = A(T)\sigma(t)^n$ we obtain

$$D(t) = C_0\left\{\int_0^t A(T)\sigma^n(t')\,dt'\right\}^{\alpha+\delta}. \tag{4}$$

As time elapses, the creep damage at some point within or on the surface of the structure would first reach the critical value, D_r, at which rupture takes place due to the non-uniform stress state. This initial rupture time, t_I, is determined in accordance with eqn (4) as

$$D_r = C_0\left\{\int_0^{t_I} A(T)\sigma^n(t')\,dt'\right\}^{\alpha+\delta}. \tag{5}$$

A rupture front then develops generally as a smooth surface, and starts propagating through the structure until the entire structure collapses at some time t_{II}. It is readily seen that the lifetime of a structure may be divided into two time intervals or stages, i.e. $0 \leqslant t < t_I$ and $t_I \leqslant t < t_{II}$. In the first stage $0 \leqslant t < t_I$, the creep damage is assumed to be less than the critical value (D_r) everywhere in the structure. In the second stage $t_I \leqslant t < t_{II}$, a rupture front Σ along which

$$D = D_r \tag{6}$$

travels through the structure and complete collapse occurs at t_{II}.

A condition on the direction of travel for the rupture front Σ may be obtained by taking the total time derivative of eqn (6). Accordingly, we obtain

$$\frac{\partial D}{\partial t} + \frac{\partial D}{\partial x_j}\frac{dx_j}{dt} = 0 \tag{7}$$

in which x_j are space coordinates.

The beam problem to be studied is depicted in Fig. 1(a). We consider a beam continuously supported by an elastic Winker foundation, which exerts a restoring force as the

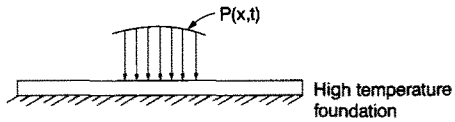

Fig. 1(a). Beam on high temperature foundation, subjected to lateral load $P(x, t)$.

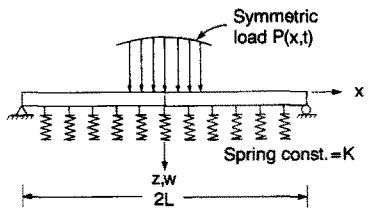

Fig. 1(b). Beam with simple end supports, elastic Winkler foundation, and symmetric load.

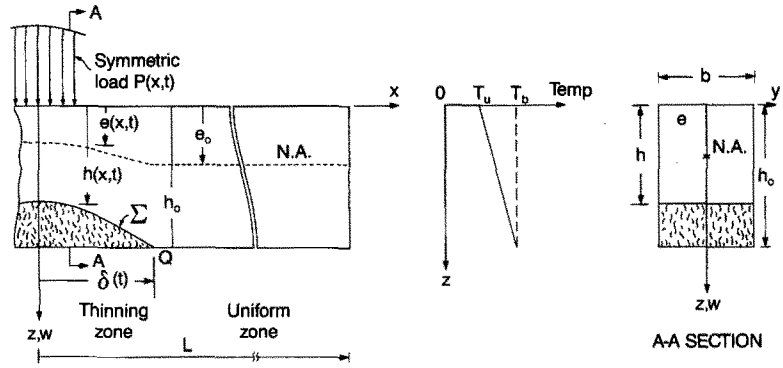

Fig. 1(c). Propagation of the rupture front and the linear temperature profile.

beam deflects under the action of a distributed lateral load. Since the foundation is at an elevated temperature, a prescribed thermal gradient is assumed to exist in the z-direction (thickness) of the beam. It is assumed that this prescribed temperature distribution through the thickness of the beam is independent of time during the deformation and rupture processes. The physical model used to analyze the problem is shown in Fig. 1(b). Here, the elastic foundation is modelled as an infinite series of infinitesimal springs with an elastic constant K in Flügge (1975), i.e. as an elastic Winkler foundation. In geophysical research this type of flexure model has recently yielded some interesting results on lithospheric flexure (McMullen *et al.*, 1981), where the temperature variation with z is due to the geothermal gradient and the Winkler foundation is due to the underlying mantle. It is our major goal here to explore the propagation of a creep rupture front in a non-isothermal beam under distributed lateral load. It will be seen later that a moving boundary problem is encountered as a consequence of this rupturing behavior (Fig. 1(c)).

2. MATHEMATICAL FORMULATION OF THE PROBLEM

In order to reduce the mathematical difficulties somewhat, we present below a series of simplifying assumptions. First, we assume that the material in the beam obeys the Norton law of steady creep, with viscosity dependent on the prescribed temperature gradient. Although the beam is of non-uniform cross-section during the second stage of damage, we assume that technical Euler–Bernoulli type beam theory is valid throughout the entire process of creep damage. We also restrict our consideration to the case of small deformations and small rotations. Furthermore, we assume that no major cracks form in the unruptured segment of the beam during the process of rupture, and thus the effects of stress concentration at crack tips are excluded from the current study. Finally, we assume that the shear stresses are negligibly small when compared with the axial stresses due to flexure. The creep deformation in the beam is assumed to be governed by Norton's law, eqn (3). Now the stress state σ may vary with time as well as with the x- and z-coordinates, and the reciprocal viscosity coefficient function, $A(z)$, is an implicit function of z via the temperature distribution (Fig. 1(c)).

The geometry of the beam is shown in Fig. 1(c). For simplicity we will consider symmetric loading in this work, and therefore only half of the span of the beam need be considered. Employing Euler–Bernoulli type beam theory we may derive the expression for stress in terms of the bending moment M as

$$\sigma = \frac{M}{\mathscr{I}_0}\left(\frac{z-e_0}{A(z)}\right)^{1/n} \tag{8}$$

where e_0 is the distance to the neutral axis (marked N.A. in Fig. 1(c)). Also, the governing equation in the bending moment M is obtained as

$$\frac{\partial^5 M}{\partial x^4\,\partial t}+K\left(\frac{M}{\mathscr{I}_0}\right)^n=\frac{\partial^3 P}{\partial x^2\,\partial t} \tag{9}$$

where P is the applied lateral load, and we have introduced the notation for flexural rigidity

$$\mathscr{I}_0=b\int_0^{h_0}\left[\frac{z'-e_0}{A(z')}\right]^{1/n} z'\,\mathrm{d}z'. \tag{10}$$

The right-hand side of eqn (9) vanishes if we assume that the applied lateral load $P(x,t)$ is expressed mathematically in the form $P_0 f(x)H(t)$, where P_0 is the maximum load at $x=0$, $f(x)$ is the symmetric shape function, and $H(t)$ represents the Heaviside unit step function. For a viscous material governed by Norton's law we have the initial condition in M as

$$\frac{\mathrm{d}^2 M(x,0^+)}{\mathrm{d}x^2}=-f(x). \tag{11}$$

For further simplicity, we also assume that the beam is simply supported at both ends and that the lateral load vanishes at both ends. Due to the symmetric nature of the problem as previously mentioned, the boundary conditions follow as

$$\frac{\partial M}{\partial x}=\frac{\partial^3 M}{\partial x^3}=0 \quad \text{at} \quad x=0; \quad \frac{\partial^2 M}{\partial x^2}=M=0 \quad \text{at} \quad x=L. \tag{12}$$

Since the axial force is zero in this problem, the distance to the neutral axis e_0 may be determined in the first stage of damage from

$$\int_0^{h_0}\left[\frac{z'-e_0}{A(z')}\right]^{1/n}\mathrm{d}z'=0. \tag{13}$$

The shear stresses in technical beam theory are usually negligibly small when compared with the axial stress. It is thus reasonable to utilize the uniaxial strain-controlled damage law. The creep damage then follows from eqn (4), which with the use of eqn (8) yields

$$D(x,z,t)=C_0\left\{\int_0^t\left[\frac{M}{\mathscr{I}_0}\right]^n(z-e_0)\,\mathrm{d}t'\right\}^{\alpha+\delta}. \tag{14}$$

Experimental evidence by Schiller *et al.* (1973–76) has shown that there is virtually no creep damage in a crystalline material under compression. Therefore, the above equation is valid only in the region $e_0 < z \leqslant h_0$ (Fig. 1(c)), while the creep damage is assumed to be identically zero in the remainder of the region.

Rupture thus starts at the point $(x,z)=(0,h_0)$, at which the tensile strain is maximum in magnitude, and then develops into a moving front which in turn causes the beam to thin (Fig. 1(c)). We shall call the region $0 \leqslant x < \delta(t)$ the thinning zone, and the remaining interval $\delta(t) \leqslant x \leqslant L$ the uniform zone for its uniform thickness. The quantities h, e, and $\mathscr{I}$, which designate the thickness, the distance to the neutral axis, and flexural rigidity within the thinning zone of the beam, are clearly functions of x and t. Governing eqn (9) with P given as $P_0 f(x)H(t)$ may now be restated in both zones as

$$\frac{\partial^5 M}{\partial x^4\,\partial t}+K\left(\frac{M}{\mathscr{I}}\right)^n=0, \quad 0 \leqslant x < \delta(t), \quad t_1 \leqslant t \tag{15a}$$

$$\frac{\partial^5 M}{\partial x^4\,\partial t}+K\left(\frac{M}{\mathscr{I}_0}\right)^n=0, \quad \delta(t) < x \leqslant L, \quad t_1 \leqslant t \tag{15b}$$

where $\mathscr{I}(x,t)$ may be obtained by replacing h_0 and e_0 in eqn (10) by $h(x,t)$ and $e(x,t)$.

It is readily seen that governing eqns (15) are subjected to a moving junction, which separates the thinning zone from the uniform zone. Note that the upper limit $h(x,t)$ and the quantity $e(x,t)$ in $\mathscr{I}(x,t)$ are unknown functions, and thus we must obtain conditions

which govern the variables h, δ, and e. It is shown (Gu, 1984) that if the rupture front Σ is prescribed as $z = h(x, t)$, eqn (7) can be rewritten as

$$\frac{\partial D}{\partial t} + \frac{\partial h}{\partial t}\frac{\partial D}{\partial z} = 0. \tag{16}$$

Substitution of eqn (14) into the above equation yields after some manipulation

$$\frac{\partial h}{\partial t} = -\left(\frac{M}{\mathscr{I}}\right)^n (h-e) \Big/ \left\{\int_0^t \left(\frac{M}{\mathscr{I}}\right)^n \mathrm{d}t'\right\}, \quad 0 \leqslant x < \delta(t), \quad t_1 \leqslant t. \tag{17}$$

The creep damage at junction point Q in Fig. 1(c) with coordinates $x = \delta(t)$ and $z = h_0$ should be equal to the critical value, D_r. Following the same procedure employed for eqn (17), the total time derivative of the damage at Q gives

$$\frac{\mathrm{d}\delta(t)}{\mathrm{d}t} = -M^n \Big/ \left\{n\int_0^t M^{n-1}\frac{\partial M}{\partial x}\,\mathrm{d}t'\right\}, \quad x = \delta(t), \quad t_1 \leqslant t. \tag{18}$$

Note that the quantity $\mathscr{I}(x, t)$ does not appear in the above equation as it is a constant at junction point Q.

Finally, differentiating eqn (13) with respect to time after replacing h_0 and e_0 by $h(x, t)$ and $e(x, t)$ we obtain

$$\frac{\partial e}{\partial t} = n\left[\frac{h-e}{A(h)}\right]^{1/n}\left(\frac{\partial h}{\partial t}\right) \Big/ \left\{\int_0^h \frac{(z'-e)^{1/n-1}}{[A(z')]^{1/n}}\,\mathrm{d}z'\right\}, \quad 0 \leqslant x < \delta(t), \quad t_1 \leqslant t \tag{19}$$

where $A(h)$ is the reciprocal viscosity function $A(z)$ evaluated at $z = h$.

We have thus obtained governing eqns (15) subjected to interface eqns (17)–(19) and we must solve these equations for the unknowns M, h, δ, and e with boundary conditions (12).

3. NUMERICAL TECHNIQUE AND RESULTS

3.1. *Solution technique*

For convenience we introduce the following non-dimensional variables:

$$\bar{t} = \frac{t}{t_1}(\bar{t}_1 = 1), \qquad \bar{e} = \frac{e}{h_0}, \qquad \bar{\delta} = \frac{\delta}{L}$$

$$\bar{x} = \frac{x}{L}(0 \leqslant \bar{x} \leqslant 1), \qquad \bar{D} = \frac{D}{D_{cr}}(0 \leqslant \bar{D} \leqslant 1)$$

$$\bar{h} = \frac{h}{h_0}(\bar{h}_0 = 1), \qquad \bar{\mathscr{I}} = \frac{\mathscr{I}}{\mathscr{I}^*}, \qquad \bar{w} = \frac{wK}{P_0}$$

$$\bar{z} = \frac{z}{h_0}(0 \leqslant \bar{z} \leqslant 1), \qquad \bar{A} = \frac{A(z)}{A(z=0)}, \qquad \bar{M} = \frac{M}{P_0 L^2}. \tag{20}$$

In the above, $\mathscr{I}^*$ represents the flexural rigidity of a beam at a uniform temperature T_u, the temperature at the upper surface of the present non-uniform beam. Thus

$$\mathscr{I}^* = \frac{nbh^{1/n+2}}{2(2n+1)[2A(z=0)]^{1/n}} \tag{21a}$$

$$\bar{\mathscr{I}} = \frac{(1+2n)2^{1/n+1}}{n} \int_0^h \left[\frac{\bar{z}'-\bar{e}}{\bar{A}(\bar{z}')}\right]^{1/n} \bar{z}' \, d\bar{z}'. \tag{21b}$$

We now follow the practice that unless otherwise noted all variables without bars appearing in this section from this point on will be dimensionless variables. In accordance with the above definitions, governing eqn (9) may be reformulated in terms of dimensionless variables as

$$\frac{\partial^5 M}{\partial x^4 \partial t} + B\left(\frac{M}{\mathscr{I}_0}\right)^n = 0 \tag{22}$$

in which we have introduced the dimensionless quantity

$$B = \frac{Kt_1 P_0^{n-1} L^{2n+2}}{\mathscr{I}_0^{*n}}. \tag{23}$$

The variables appearing on the right-hand side of eqn (23) are all in dimensional form, and $\mathscr{I}_0^*$ is evaluated by setting $h = h_0$ in eqn (21a). Note that the quantity B will be the key parameter in the present non-dimensional study.

Employing the same techniques presented in McMullen *et al.* (1981), we may eliminate the spatial partial derivative appearing in eqn (22) for the first stage. We thus obtain the integro-differential equations

$$\frac{\partial M}{\partial t} = \frac{B}{6}\left\{\int_0^x F(x,x')\left(\frac{M}{\mathscr{I}_0}\right)^n dx' + \int_0^1 G(x,x')\left(\frac{M}{\mathscr{I}_0}\right)^n dx'\right\} \tag{24a}$$

where

$$F(x,x') = -(x-x')^3 \tag{24b}$$

$$G(x,x') = 3x^2 - 3x^2x' - x'^3 + 3x'^2 - 2. \tag{24c}$$

Here we employ a discretization scheme using the method of lines in space. It follows that

$$\frac{\partial M_i}{\partial t} = \frac{B}{6}\left\{\int_0^{x_i} F(x_i,x')\left(\frac{M}{\mathscr{I}_0}\right)^n dx' + \int_0^1 G(x_i,x')\left(\frac{M}{\mathscr{I}_0}\right)^n dx'\right\}, \quad i = 1,2,\ldots,N_2+1 \tag{25}$$

where

$$x_i = (i-1)\Delta x = \frac{1}{N_2}(i-1).$$

Note that N_2 designates the number of spatial increments. Evaluating the integrals by the Newton–Cotes formulas, we thus obtain a system of ODEs which may be solved by Gear's stiff ODE algorithm (Gear, 1967). The result obtained above furnishes the solution in the first stage of damage, and provides the initial data for the second stage of damage.

Returning now to eqns (15), we may again integrate out the spatial derivatives to obtain for both zones in the second stage

$$\frac{\partial M}{\partial t} = \frac{B}{6}\left\{\int_0^x F(x,x')\left(\frac{M}{\mathscr{J}}\right)^n \mathrm{d}x' + \int_0^{\delta(t)} G(x,x')\left(\frac{M}{\mathscr{J}}\right)^n \mathrm{d}x' + \int_{\delta(t)}^1 G(x,x')\left(\frac{M}{\mathscr{J}_0}\right)^n \mathrm{d}x'\right\}, \quad 0 \leqslant x < \delta(t), \quad 1 \leqslant t \tag{26a}$$

$$\frac{\partial M}{\partial t} = \frac{B}{6}\left\{\int_0^{\delta(t)} F(x,x')\left(\frac{M}{\mathscr{J}}\right)^n \mathrm{d}x' + \int_{\delta(t)}^x F(x,x')\left(\frac{M}{\mathscr{J}_0}\right)^n \mathrm{d}x' + \int_0^{\delta(t)} G(x,x')\left(\frac{M}{\mathscr{J}}\right)^n \mathrm{d}x' + \int_{\delta(t)}^1 G(x,x')\left(\frac{M}{\mathscr{J}_0}\right)^n \mathrm{d}x'\right\}, \quad \delta(t) \leqslant x < 1, \quad 1 \leqslant t. \tag{26b}$$

Note that we have used the fact that the bending moment, shear force, deflection, and slope of the beam are all continuous at the junction point.

In order to mathematically fix the moving junction and the limits of integration appearing in eqns (26), we employ the concept of Landau's transformation (Landau, 1950), and introduce the variable changes

$$\zeta = \frac{x}{\delta(t)}, \quad \text{for thinning zone} \quad 0 \leqslant x < \delta(t) \tag{27a}$$

$$\eta = \frac{x-\delta(t)}{1-\delta(t)}, \quad \text{for uniform zone} \quad \delta(t) \leqslant x \leqslant 1. \tag{27b}$$

With the use of the chain rule and the definition of a substantial time derivative $\mathrm{D}(\ )/\mathrm{D}t$, the transformed governing equations are obtained for both zones as

$$\frac{\mathrm{D}M}{\mathrm{D}t} = \frac{\zeta}{\delta(t)}\frac{\mathrm{d}\delta(t)}{\mathrm{d}t}\frac{\partial M}{\partial \zeta} + \frac{B}{6}\left\{\delta(t)\int_0^\zeta F(\zeta,\zeta')\left(\frac{M}{\mathscr{J}}\right)^n \mathrm{d}\zeta' + \delta(t)\int_0^1 G(\zeta,\zeta')\left(\frac{M}{\mathscr{J}}\right)^n \mathrm{d}\zeta' + [1-\delta(t)]\int_0^1 G(\zeta,\eta')\left(\frac{M}{\mathscr{J}_0}\right)^n \mathrm{d}\eta'\right\}, \quad 0 \leqslant \zeta < 1, \quad 1 \leqslant t \tag{28a}$$

$$\frac{\mathrm{D}M}{\mathrm{D}t} = \frac{1-\eta}{1-\delta(t)}\frac{\mathrm{d}\delta(t)}{\mathrm{d}t}\frac{\partial M}{\partial \eta} + \frac{B}{6}\left\{\delta(t)\int_0^1 F(\eta,\zeta')\left(\frac{M}{\mathscr{J}}\right)^n \mathrm{d}\zeta' + [1-\delta(t)]\int_0^\eta F(\eta,\eta')\left(\frac{M}{\mathscr{J}_0}\right)^n \mathrm{d}\eta' + \delta(t)\int_0^1 G(\eta,\zeta')\left(\frac{M}{\mathscr{J}}\right)^n \mathrm{d}\zeta' + [1-\delta(t)]\int_0^1 G(\eta,\eta')\left(\frac{M}{\mathscr{J}_0}\right)^n \mathrm{d}\eta'\right\}, \quad 0 \leqslant \eta \leqslant 1, \quad 1 \leqslant t. \tag{28b}$$

Similarly, an application of Landau's transformation to interface eqns (17) and (19) yields

$$\frac{\mathrm{D}h}{\mathrm{D}t} = \frac{\zeta}{\delta(t)}\frac{\mathrm{d}\delta(t)}{\mathrm{d}t}\frac{\partial h}{\partial \zeta} - \left(\frac{M}{\mathscr{J}}\right)^n (h-e)\Big/\left\{\int_0^t \left[\frac{M}{\mathscr{J}}\right]^n \mathrm{d}t'\right\}, \quad 0 \leqslant \zeta < 1, \quad 1 \leqslant t \tag{29}$$

$$\frac{\mathrm{D}e}{\mathrm{D}t} = \frac{\zeta}{\delta(t)}\frac{\mathrm{d}\delta(t)}{\mathrm{d}t}\frac{\partial e}{\partial \zeta} + n\left[\frac{\mathrm{D}h}{\mathrm{D}t} - \frac{\zeta}{\delta(t)}\frac{\mathrm{d}\delta(t)}{\mathrm{d}t}\frac{\partial h}{\partial \zeta}\right]\left[\frac{h-e}{A(h)}\right]^{1/n}\Big/\left\{\int_0^h \frac{(z'-e)^{1/n-1}}{[A(z')]^{1/n}}\,\mathrm{d}z'\right\}, \quad 0 \leqslant \zeta < 1, \quad 1 \leqslant t. \tag{30}$$

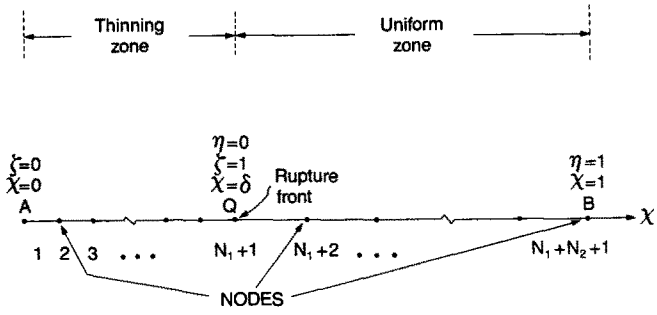

Fig. 2. Variable network in the second stage of creep damage.

The transformed interface eqn (18) has the slightly different form

$$\frac{\mathrm{d}\delta(t)}{\mathrm{d}t} = -\delta(t)M^n \Big/ \left\{ n \int_0^t M^{n-1} \frac{\partial M}{\partial \zeta}\, \mathrm{d}t' \right\}, \quad \zeta = 1, \quad 1 \leqslant t \tag{31}$$

since $\delta(t)$ involves only the single variable t. It should be noted that fixing the moving junction unfortunately leads to governing equations of even more complicated form, which may be solved by the following numerical scheme.

First, the method of lines in space in Furzeland (1979) is utilized to eliminate the spatial derivatives from the above integro-differential equations in accordance with the discretization scheme shown in Fig. 2. Accordingly, we employ the central finite difference approximations for the interior points and one-sided three point formulas for the end points A, B and junction point Q (Fig. 2). As a result, eqns (28)–(31) yield the following:

$$\frac{\mathrm{d}\delta(t)}{\mathrm{d}t} = -2\Delta\zeta\delta(t)M_i^n \Big/ \left\{ n \int_0^t M_i^{n-1}[M_{i-2} - 4M_{i-1} + M_i]\, \mathrm{d}t' \right\}, \quad i = N_1 + 1 \tag{32}$$

$$\frac{\mathrm{D}M_i}{\mathrm{D}t} = \frac{\zeta_i}{2\Delta\zeta\delta(t)} \frac{\mathrm{d}\delta(t)}{\mathrm{d}t}[M_{i+1} + M_{i-1}] + \frac{B}{6}\left\{ \delta(t) \int_0^{\zeta_i} F(\zeta_i, \zeta') \left(\frac{M}{\mathscr{J}}\right)^n \mathrm{d}\zeta' \right.$$

$$\left. + \delta(t) \int_0^1 G(\zeta_i, \zeta') \left(\frac{M}{\mathscr{J}}\right)^n \mathrm{d}\zeta' + [1 - \delta(t)] \int_0^1 G(\zeta_i, \eta') \left(\frac{M}{\mathscr{J}_0}\right)^n \mathrm{d}\eta' \right\}, \quad i = 1, 2, \ldots, N_1 \tag{33a}$$

$$\frac{\mathrm{D}M_i}{\mathrm{D}t} = \frac{1 - \eta_i}{2\Delta\eta[1 - \delta(t)]} \frac{\mathrm{d}\delta(t)}{\mathrm{d}t}[M_{i+1} - M_{i-1}] + \frac{B}{6}\left\{ \delta(t) \int_0^1 F(\eta_i, \zeta') \left(\frac{M}{\mathscr{J}}\right)^n \mathrm{d}\zeta' \right.$$

$$+ [1 - \delta(t)] \int_0^{\eta_i} F(\eta_i, \eta') \left(\frac{M}{\mathscr{J}_0}\right)^n \mathrm{d}\eta' + \delta(t) \int_0^1 G(\eta_i, \zeta') \left(\frac{M}{\mathscr{J}}\right)^n \mathrm{d}\zeta'$$

$$\left. + [1 - \delta(t)] \int_0^1 G(\eta_i, \eta') \left(\frac{M}{\mathscr{J}_0}\right)^n \mathrm{d}\eta' \right\}, \quad i = N_1 + 1, N_1 + 2, \ldots, N_1 + N_2 + 1 \tag{33b}$$

$$\frac{\mathrm{D}h_i}{\mathrm{D}t} = \frac{\zeta_i}{2\Delta\zeta\delta(t)} \frac{\mathrm{d}\delta(t)}{\mathrm{d}t}[h_{i+1} - h_{i-1}] - \left(\frac{M_i}{\mathscr{J}_i}\right)^n (h_i - e_i) \Big/ \left\{ \int_0^t \left(\frac{M_i}{\mathscr{J}_i}\right)^n \mathrm{d}t' \right\},$$

$$i = 1, 2, \ldots, N_1 + 1 \tag{34}$$

$$\frac{\mathrm{D}e_i}{\mathrm{D}t} = \frac{\zeta_i}{2\Delta\zeta\delta(t)} \frac{\mathrm{d}\delta(t)}{\mathrm{d}t}[e_{i+1} - e_{i-1}] + n\left[\frac{\mathrm{D}h_i}{\mathrm{D}t} - \frac{\zeta_i}{2\Delta\zeta\delta(t)} \frac{\mathrm{d}\delta(t)}{\mathrm{d}t}(h_{i+1} - h_{i-1})\right]\left[\frac{h_i - e_i}{A(h_i)}\right]^{1/n} \Big/ \left\{ \int_0^{h_i} \frac{(z' - e_i)^{1/n - 1}}{[A(z')]^{1/n}}\, \mathrm{d}z' \right\}, \quad i = 1, 2, \ldots, N_1 + 1. \tag{35}$$

In the above

$$\zeta_i = (i-1)\Delta\zeta = \frac{1}{N_1}(i-1), \quad i = 1, 2, \ldots, N_1$$

$$\eta_i = (i-N_1-1)\Delta\eta = \frac{1}{N_2}(i-N_1-1), \quad i = N_1+1, N_1+2, \ldots, N_1+N_2+1$$

$$\Delta\zeta = \frac{1}{N_1}, \quad \Delta\eta = \frac{1}{N_2}$$

and N_1, N_2 designate, respectively, the number of spatial increments in the thinning zone and uniform zone, and $\mathscr{I}_i$ is obtained by setting $h = h_i$ in eqn (21b). Note that Dh/Dt and De/Dt vanish at the junction point, since at any instant we always have $h = 1$ and $e = e_0$ at this point.

The integrals appearing in the above set of equations were evaluated by use of the Newton–Cotes formulas. We thereby obtained a large system of $3N_1+N_2+4$ ordinary differential equations. A computer program was developed first to solve eqn (13) for e_0 and then to solve eqn (25) for the M_i's using the initial bending moment function (see Section 3.2) as the initial condition. We then used these results along with $h_i = 1$, $e_i = e_0$, $\delta = 0$ as the initial conditions to solve the system of ODEs, eqns (32)–(35). It is also useful to compute the deflection of the beam. This can be accomplished by the same solution technique used for the bending moment. For the sake of brevity, the resulting equations will not be presented here. An even larger system of $4N_1+2N_2+5$ ODEs is obtained in this case. A high accuracy yet costly numerical algorithm, i.e. Gear's stiff ODE algorithm, was used to solve this system.

3.2. *Solutions and discussion*

Our attention is first directed to a special case in which closed form solutions exist. Thus, let us delete the elastic Winkler foundation and also consider a beam with a uniform temperature distribution equal to T_u (a dimensional quantity). Under such circumstances, the bending moment M remains constant in time, and the neutral axis coincides with the centroidal axis owing to the homogeneous nature of the material properties. Moreover, we choose the dimensionless quantities $e = h/2$, $A(z) = 1$, and $\mathscr{I} = h^{1/n+2}$. The dimensionless governing equations for h, e (see eqns (17) and (19)) in the thinning zone ($0 \leqslant x < \delta(t)$) follow for this special case as

$$\frac{\partial h}{\partial t} = -\frac{h^{-2n}}{2\int_0^t h^{-1-2n}\,\mathrm{d}t'}, \quad 1 \leqslant t \tag{36a}$$

$$\frac{\partial e}{\partial t} = 2\frac{\partial h}{\partial t}, \quad 1 \leqslant t \tag{36b}$$

and that for $\delta(t)$ becomes

$$\frac{\mathrm{d}\delta(t)}{\mathrm{d}t} = -\frac{M}{nt\dfrac{\partial M}{\partial x}}, \quad x = \delta(t), \quad 1 \leqslant t. \tag{36c}$$

Note that these equations may be solved consecutively and that eqns (36a) and (36b) include neither the x variable nor the input load function $P(x, t)$ explicitly. Physically, eqn (36b) indicates that although $2e_0 = h_0 = 1$ initially, both quantities will be equal to zero at the instant the beam collapses. After eliminating the integral via differentiation, eqn (36a)

may be rewritten as

$$\frac{\partial}{\partial t}\left[\frac{\partial h}{\partial t}\cdot h^{2n-2}\right]=0 \tag{37}$$

which may be solved analytically with the initial conditions

$$h=1 \quad \text{at} \quad t=t_1; \quad \frac{\partial h}{\partial t}=-\frac{1}{2t_1} \quad \text{at} \quad t=t_1.$$

Here $t_1=t_1(x)$ designates the time required for a material point with coordinates $(x, 1)$ to reach the critical state. The second initial condition in the above was obtained by setting $t=t_1$ and $h=1$ in eqn (36a). The solution to eqn (37) is then obtained as

$$\frac{t}{t_1(x)}=\frac{2}{1-2n}h^{2n-1}-\frac{1+2n}{1-2n}, \quad 0\leqslant x<\delta(t), \quad 1\leqslant t \tag{38}$$

which is identical to the result derived in Kachanov (1961).

The solution to eqn (36b) for e then follows directly from eqn (38). Here $t_1(x)$ may be expressed in terms of the bending moment $M(x)$. Since the point $(0, 1)$ reaches the critical state at time $t=1$ while the point $(x, 1)$ ruptures at time $t=t_1(x)$, it follows from eqns (5) and (8) that

$$t_1(x)=\left(\frac{M_0}{M}\right)^n. \tag{39}$$

Here, M_0 and M represent the bending moments at points $x=0$ and x, respectively. Equation (38) thus becomes

$$\left(\frac{M}{M_0}\right)^n t=\frac{2}{1-2n}h^{2n-1}-\frac{1+2n}{1-2n}, \quad 0\leqslant x<\delta(t), \quad 1\leqslant t. \tag{40}$$

Although differential eqn (36a) does not explicitly involve the variable x and the bending moment M, its solution (40) is seen to be directly related to M.

The function $t_1(x)$ in eqn (39) may be inverted in the simple case that the bending moment $M(x)$ is monotonic in nature. In fact, for such a simple case the constraint on the moving junction, $x=\delta(t)$, is invertible and is physically equivalent after inversion to $t=t_1(x)$. Consequently, with the use of eqn (39), eqn (36c) attains the alternate form

$$\frac{\mathrm{d}\delta(t)}{\mathrm{d}t}=-\frac{M^{n+1}}{nM_0^n\dfrac{\partial M}{\partial x}}, \quad x=\delta(t), \quad 1\leqslant t. \tag{41}$$

Consider for the moment a very simple case in which a point load is applied on the beam at $x=0$, giving the bending moment of $M=M_0(1-x)$. Equation (41) becomes

$$\frac{\mathrm{d}\delta(t)}{\mathrm{d}t}=\frac{1}{n}[1-\delta(t)]^{n+1}, \quad 1\leqslant t.$$

With the initial condition that $\delta(1)=0$, the above equation yields the solution

$$\delta(t)=1-t^{-1/n}, \quad 1\leqslant t. \tag{42}$$

Note that solution (42) is also obtainable from solution (40) by setting $h = 1$ and using expression $M = M_0(1-x)$.

We thus turn our attention to the original problem, containing in general both the Winkler term and a temperature gradient. The temperature in the beam is assumed to be linearly distributed in the z-direction in accordance with $T = T_u + (T_b - T_u)z$, $0 \leqslant z \leqslant 1$ (Fig. 1(c)). Here the dimensional surface and bottom temperatures, T_u and T_b, are chosen as 300 and 360 K, respectively. Also, we use for the creep activation energy the dimensional value 0.112×10^6 J mol^{-1}. Note that because of the non-dimensional form of our governing equations it was not necessary to stipulate a specific material. Finally the number of increments chosen in the present beam problem were $N_1 = 5$ for the thinning zone, and $N_2 = 10$ for the uniform zone, which yield a total of 29 ODEs, or 45 if the equations for deflection are also included. In order to limit the complexity of this non-linear problem, only the uniformly applied load is considered here. In this case, the shape function of the applied load is simply $f(x) = 1$, $0 \leqslant x \leqslant 1$. The initial bending moment function $M(x, 0^+)$ is obtainable from eqns (11) and (12), and is given as $M(x, 0^+) = (x^2 - 1)/2$, which will be used as the initial condition for eqn (25).

The results we shall present may be separated into two groups, i.e. those with and without the foundation. In the latter case, we have from eqn (23) $B = 0$, and note that here the bending moment is independent of time. (For this case, we did not calculate the deflection of the beam.) Figures 3(a) and (b) display the propagating rupture front for $B = 0$ in the second stage of damage for $n = 3$ and 5, respectively. In these figures the depth and axial coordinates z, x of the beam are given in non-dimensional form. The sequence of curves inside the beam traces the propagation of the rupture front as time elapses. The $\delta(t)$ function is given by the distance along the bottom surface ($z = 1$) from the point $x = 0$ to the intersection of the curve for time t with the bottom surface. Note

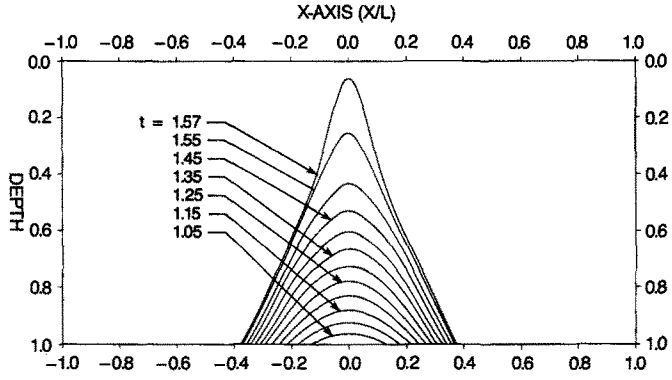

Fig. 3(a). Propagation of rupture front in a beam with no Winkler foundation, $B = 0$ and $n = 3$.

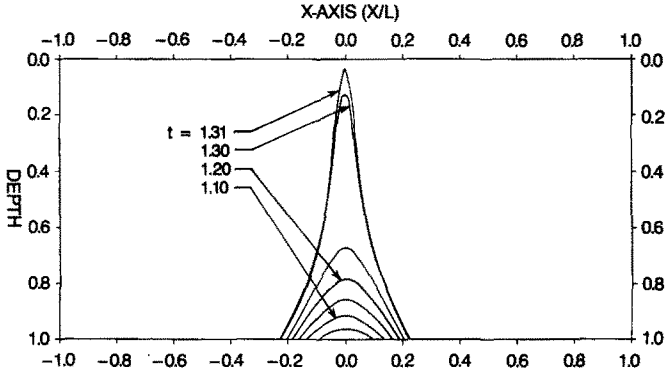

Fig. 3(b). Propagation of rupture front in a beam with no Winkler foundation, $B = 0$ and $n = 5$.

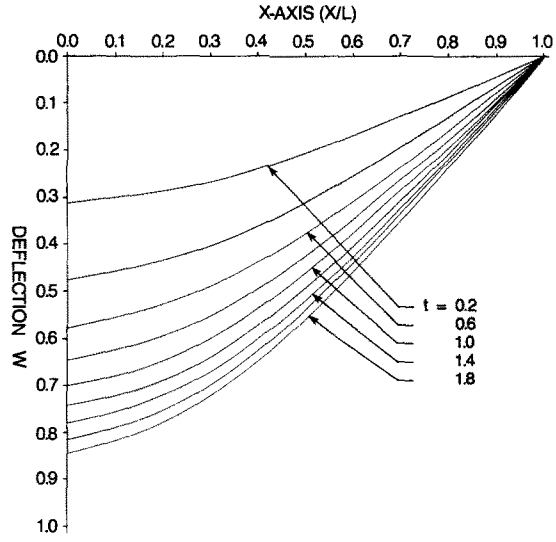

Fig. 4(a). Non-dimensional deflection of a beam resting on Winkler foundation, $B = 1$, $n = 3$, $T_b = 360\,\text{K}$ and $T_u = 300\,\text{K}$.

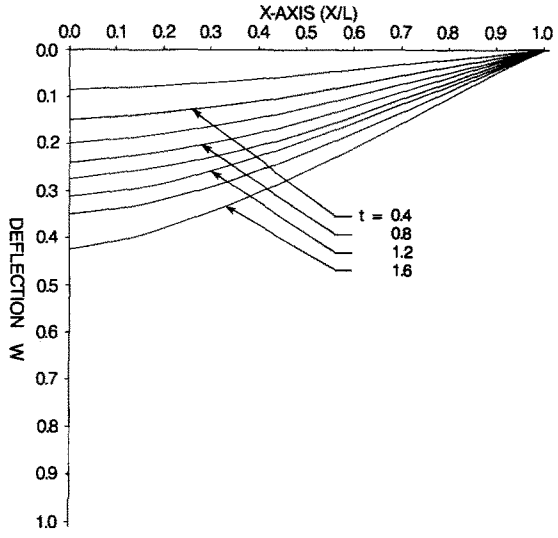

Fig. 4(b). Non-dimensional deflection of a beam resting on Winkler foundation, $B = 1$, $n = 5$, $T_b = 360\,\text{K}$ and $T_u = 300\,\text{K}$.

that the beam of $n = 3$ material exhibits a wider thinning zone than does the beam of $n = 5$ material. It would appear that the rupture front of the $n = 5$ beam propagates faster than that of the $n = 3$ beam. But this observation is made for a non-dimensional time scale and will not necessarily follow for dimensional time. Each set of these curves for a parameter n required about 1 min of computer time (CPU) on a CDC CYBER 173.

We now turn to the general case with the Winkler foundation present. The dimensionless parameter B contains a group of constants including the spring constant of the foundation, applied load, geometry and material properties of the beam, and is considered arbitrary in the present non-dimensional study. Here we chose for illustration the value $B = 1$ which requires that the numerator and denominator in eqn (23) be of the same order. In addition to the bending moment M, we also compute the deflection w for this case. Due to the complicated nature of the large system of governing ODEs, a considerable amount of computer time was required to complete one run for a specific value of n. Thus we limited the computer time to 1000 s (about 16.7 min) per run, and accordingly obtained a reasonable number of solution curves for time steps in the early part of the second stage of damage.

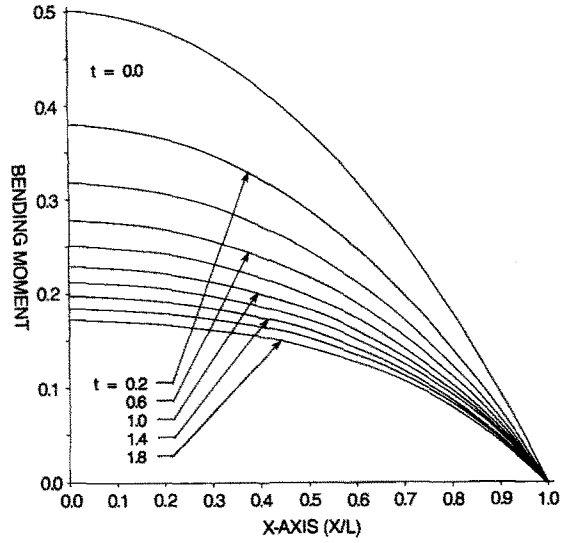

Fig. 5(a). Non-dimensional bending moment along a beam on Winkler foundation, $B = 1$, $n = 3$, $T_b = 360\,\text{K}$ and $T_u = 300\,\text{K}$.

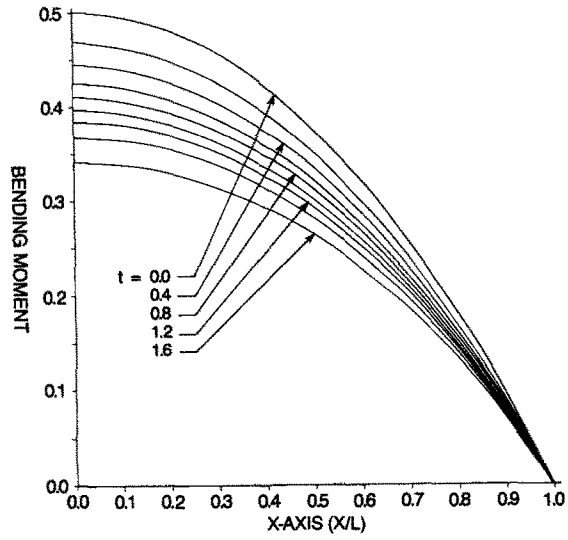

Fig. 5(b). Non-dimensional bending moment along a beam on Winkler foundation, $B = 1$, $n = 5$, $T_b = 360\,\text{K}$ and $T_u = 300\,\text{K}$.

Figures 4(a) and (b) give respectively the non-dimensional deflection of the beam for values 3 and 5 for the stress power n. Since the chosen load is uniformly distributed, these curves do not exhibit the characteristic "uplift" which often occurs under centrally concentrated loads or point loads on a beam with a Winkler foundation as shown in Flügge (1975) and McMullen *et al.* (1981). According to the flexural model presented in McMullen *et al.* (1981), the deflections of a beam which experiences no damage approaches an asymptotic limit as the time tends to infinity. However, no asymptotic deflection solution exists in the present problem, since damage causes the beam to thin and accordingly the deflection is unbounded. This may readily be seen in Fig. 4(b), in which the increment of beam deflection is clearly increasing in the final few time steps shown. Although we have used Norton's steady creep law, to describe the creep behavior of the material, the nature of the deflection shown in Fig. 4(b) is similar in form to the typical creep curve with its three stages of creep. Such behavior coincides with the recent experimental investigations

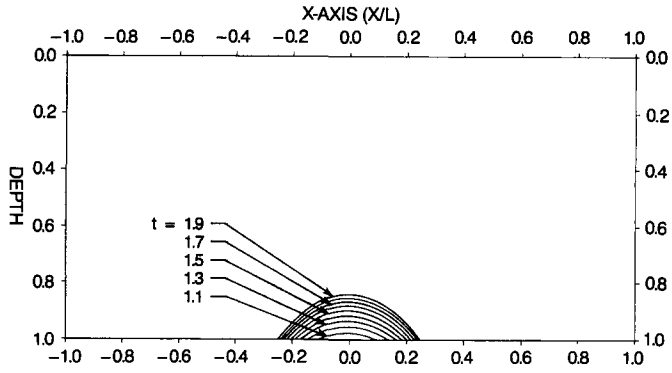

Fig. 6(a). Propagation of rupture front in a beam on Winkler foundation, $B = 1$, $n = 3$, $T_b = 360\,\text{K}$ and $T_u = 300\,\text{K}$.

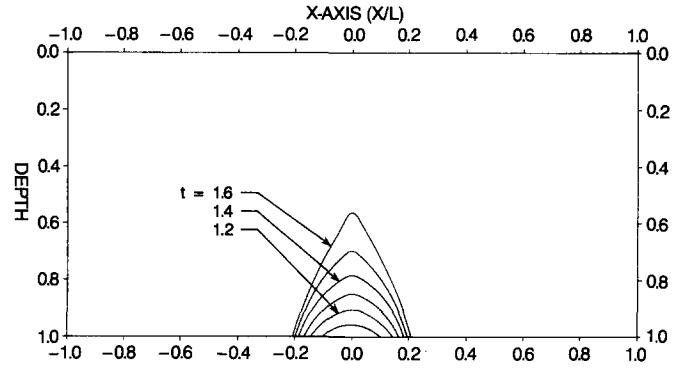

Fig. 6(b). Propagation of rupture front in a beam on Winkler foundation, $B = 1$, $n = 5$, $T_b = 360\,\text{K}$ and $T_u = 300\,\text{K}$.

by Radhakrishnan and McEvily (1980a, b) in which a beam with a deep notch was subjected to a uniform temperature and point load. This can be explained by the fact that as the beam starts thinning the remaining material carries the same load but with greater stress.

In McMullen *et al.* (1981) where no damage was included, it was noted that the bending moment relaxes after the load is applied and approaches zero as time tends to infinity. Figures 5(a) and (b) exhibit this same relaxation of the bending moment in the more general case where damage causes the beam to thin. Furthermore, Fig. 5(b) shows that the relaxation of the bending moment accelerates in the final few time steps shown; it is believed that Fig. 5(a) would also do the same if the computer time had been extended. Since the lifetime of the beam is finite, the beam should collapse before the bending moment vanishes. Figures 6(a) and (b) display the propagating rupture front for $B = 1$ with $n = 3$ and 5, respectively. As in the $B = 0$ case, the rupture fronts in the present case have sharper profiles in the $n = 5$ beam than in the $n = 3$ beam. The rupture front for the $n = 5$ beam propagates faster than that for the $n = 3$ beam relative to the non-dimensional time scale. We also point out that the numerical scheme for the system of ODEs presented in the previous section is stiffer for $n = 5$ than that for $n = 3$, since within the chosen limit of computing time (1000 s) the final time step reached was $t = 1.90$ for the case of $n = 3$ and only $t = 1.60$ for the case of $n = 5$. It should be noted that the results displayed may contain some numerical error in the later time intervals, since we are restricted by the limitations of infinitesimal strain and small rotations. Although we have formulated the problem in an idealized manner, a significant amount of mathematical difficulty was still encountered. If one attempts to relax some of the assumptions imposed, the complexity of the problem could increase greatly and possibly preclude a successful numerical analysis.

We have presented in this paper a continuum mechanical creep rupture analysis for a beam resting on a high temperature elastic Winkler foundation, using a previously proposed strain-controlled creep damage law. Although the analysis has been carried out in non-dimensional form for convenience, some of the material properties used in the creep law and in the creep damage law may be found in the references (Cozzarelli and Bernasconi, 1981). Experimental validation of the present analysis has not yet been attempted, but it should not be difficult due to the simplicity of the analyzed geometry. We also note that a finite difference numerical technique has been employed to solve the present moving boundary problem. A finite element code capable of handling creep deformations and moving boundaries may also be used for this analysis.

REFERENCES

Belloni, G., Bernasconi, G. and Piatti, G. (1977). Damage and rupture in AISI 310 austenitic steel. *Meccanica* **12,** 84–96.

Belloni, G., Bernasconi, G. and Piatti, G. (1980). Creep damage models. In *Creep in Engineering Materials and Structures* (Edited by G. Bernasconi and G. Piatti), Chap. 8, pp. 195–229. Applied Science, London.

Cozzarelli, F. A. and Bernasconi, G. (1981). Nonlinear creep damage under one-dimensional variable tensile stress. *Int. J. Non-linear Mech.* **16**(1), 27–38.

Flügge, W. (1975). *Viscoelasticity*, 2nd Revised Edn. Springer, New York.

Furzeland, R. M. (1979). Analysis and computer packages for Stefan problems. Internal Report, Oxford University Computing Laboratory.

Gear, C. W. (1967). Numerical integration of stiff ordinary differential equations. Report No. 221, Department of Computer Science, University of Illinois.

Gu, R. J. (1984). Strain-controlled creep rupture in non-isothermal materials. Ph.D. Dissertation, State University of New York at Buffalo.

Gu, R. J. and Cozzarelli, F. A. (1988). The strain-controlled creep damage law and its application to the rupture analysis of thick-wall tubes. *Int. J. Non-linear Mech.* **23**(2), 147–165.

Kachanov, L. M. (1961). Rupture time under creep conditions. In *Problems of Continuum Mechanics, Contributions in Honor of Seventieth Birthday of N. I. Muskhelishville* (Edited by J. R. M. Radok), pp. 202–218. SIAM, Philadelphia.

Landau, H. G. (1950). Heat conductions in a melting solid. *Q. Appl. Math.* **8,** 81–94.

McMullen, R. J., Hodge, D. S. and Cozzarelli, F. A. (1981). A technique for incorporating geothermal gradients and nonlinear creep into lithospheric flexure models. *J. Geophys. Res.* **86,** 1745–1753.

Piatti, G., Lubek, R. and Matera, R. (1977). The measurement of small density variations in solids. JRC Tech. Note N.I.77.6 173/2. 10.1/3.

Radhakrishnan, V. M. and McEvily, A. J. (1980a). A critical analysis of crack growth in creep. *Trans. ASME J. Engng Mater. Technol.* **102,** 200–206.

Radhakrishnan, V. M. and McEvily, A. J. (1980b). Effect of temperature on creep crack growth. *Trans. ASME J. Engng Mater. Technol.* **102,** 350 355.

Schiller, P., Boerman, D., Fenici, P., Matera, R., Pellegrini, G., Piatti, G. and Ruedl, E. (1973–76). Testing and modeling of mechanical properties of metals. In *Highlights of Materials Science*, EUR-5508, pp. 53–67.

Woodford, D. A. (1969). A parametric approach to creep damage. *Met. Sci. J.* **3,** 50–53.